ELSEVIER

Journal of Photochemistry and Photobiology A: Chemistry 95 (1996) 51–59

Journal of PHOTOCHEMISTRY AND PHOTOBIOLOGY A: CHEMISTRY

Solvent effects on the electron transfer reactions in supramolecular systems

J. Najbar [a,b], M. Tachiya [b]

[a] *Department of Physical Chemistry and Electrochemistry, Jagiellonian University, 3 Ingardena, 30-060 Krakow, Poland*
[b] *Department of Physical Chemistry, National Institute of Materials and Chemical Research, Tsukuba, Ibaraki 305, Japan*

Abstract

The kinetics of charge separation due to the outer-sphere electron transfer processes in triad systems D–A–A in a polar environment were investigated using the stochastic Liouville equations. The solvation phenomena of the triad system in the different electronic states were described using Green's functions in two mutually correlated reaction coordinates and their auto- and cross-correlation functions. The coupling between the sequential and superexchange processes in the triad system was investigated.

Keywords: Solvent effects; Electron transfer reactions; Supramolecular systems

1. Introduction

In recent years, much effort has been made to model the electron transfer processes in triad systems related to photosynthetic reaction centres [1–10]. In the photosynthetic reaction centre of *Rhodopseudomonas viridis*, the bacteriochlorophyll special pair donor (P) is initially excited. An electron is transferred from P* to a distant bacteriopheophytin (H_L). These two subunits are bridged by bacteriochlorophyll monomer (B_L), which can function as a real electron acceptor or can contribute to effective electronic coupling between the special pair dimer (P*) and bacteriopheophytin (H_L). The importance of the relative contributions of the sequential, two-step charge separation and the direct process due to superexchange has been the subject of many theoretical considerations and experimental research [1–4,8].

Hu and Mukamel [6,7] developed a unified theory of electron transfer in the triad system using the density matrix method. The approach exploits an analogy between the electron transfer processes in multicentre donor–acceptor systems and non-linear optical processes and the underlying dynamics contributing to the optical lineshapes [11–17]. In particular, the electron transfer processes in the triad system are analogous to optical pump-probe experiments. They solved the Liouville equation for the density matrix using the perturbational expansion in the powers of the coupling constants V_{lk} and the Liouville space Green's functions to describe the system dynamics. The dynamics are described in terms of the coordinate auto-correlation functions and corresponding cross-correlation functions. They did not invoke directly two-dimensional potential energy surfaces for the triad system. In this paper, we show that using the concept of a two-dimensional energy surface, we can recover the formal results of the Hu and Mukamel theory [6,7] in a form convenient for analysis of the couplings between different processes. The role of the correlation between two solvent polarization coordinates can be evaluated easily in the present approach.

An important question for the evaluation of the electron transfer rates is the correlation between the fluctuations in the two energy gaps between the three electronic states. The energy gaps are an obvious choice for the reaction coordinates [3,6,10,18,19]. Their fluctuations are due to intramolecular nuclear motions and outer-sphere solvent nuclear motions. The changes in the energy level separations due to solvent fluctuations can be accounted for by the difference between the electrostatic interactions of the solvent molecules with the donor and acceptor subunits of the supramolecular system [1,3,18]. The correlation of the solvent polarization coordinates is a simple consequence of the fact that each polar molecule contributes simultaneously to all electrostatic energy differences in the triad system. Recently, using the variational method, the potential energy functions in the two solvent polarization coordinates have been derived within the framework of the dielectric continuum approximation [10,18,19]. The correlation between the two solvent polarization coordinates can be simply related to the geometrical arrangement of the subunits forming the triad system. The coordinate correlation coefficient can also be given in terms

SSDI 1010-6030(95)04232-6

of the three reorganization energies characterizing the three electron transfer processes in the triad system [19].

Tang et al. [20–23] have applied the stochastic Liouville equations to solve the problem of electron transfer between three electronic states using a single solvent polarization coordinate, extending the original Zusman theory of outer-sphere electron transfer in the two-level system. Recently, Tang and Norris [9] applied the Liouville equation approach to the triad system using two non-correlated solvent polarization coordinates. However, the potential energy functions applied in Ref. [9] are not consistent with linear response theory. The horizontal displacements of the potential energy surfaces and the harmonic force constants are considered as independent quantities. This results in the rotation of the directions of the surface intersections introducing additional couplings. More direct effects resulting from the dependence of the potential energy functions on the coordinate correlation are missing in their approach. Within the framework of the linear response theory, the reorganization energies simultaneously determine the shape of the potential energy surfaces and their horizontal displacements. The corresponding relations were recently discussed in Refs. [24] and [25] for the single reaction coordinate and in Refs. [10], [18] and [19] for the triad system. It has been shown that there are three possibilities of selection of the two solvent polarization coordinates for the triad system.

The two solvent polarization coordinates and their correlation have been qualitatively considered in several papers [5,9,26]. The most precise information concerning the solvation thermodynamics as well as the solvation dynamics is obtained from molecular dynamics simulations. Extensive molecular dynamics simulations for the photosynthetic reaction centre of *Rhodopseudomonas viridis* have been performed by Marchi and coworkers [3,4]. In Ref. [3], a special choice of solvation coordinates has been used (linear combination of the energy level differences) so that the two coordinates are orthogonal at $t = 0$. Their calculations have shown that the reaction coordinates are approximately orthogonal in all the time domain. The simulations by Marchi et al. [3] show a high degree of coordinate correlation. The correlation coefficients derived from the results obtained by Marchi et al. [3] are independent of the rescaling applied for the reorganization energies.

The purpose of this paper is to analyse the non-adiabatic electron transfer processes in the triad system using the potential energy functions in the two correlated solvent polarization coordinates. The dynamics of the system are described using the stochastic Liouville equation. The solvation dynamics are described in terms of Green's functions which depend on the auto- and cross-correlation functions of the solvent polarization coordinates.

2. Solvation dynamics in the two-dimensional case

The influence of solvent polarization on the electron transfer processes in the triad system can be described in terms of two reaction coordinates. Each coordinate is related to the electrostatic energy difference for the interaction between the polar solvent molecules and the two subunits involved in the electron transfer step under consideration. For the A–B–C triad, we select the central subunit B as the subunit common to the two solvent polarization coordinates. We should mention that in some applications the subunit A is taken as reference for the two solvent polarization coordinates.

The diabatic energy surface in the solvation coordinates for the initial neutral state is given by [18]

$$U_1(q_1,q_2) = \frac{1}{2(1-\rho^2)}\left(\frac{q_1^2}{2\lambda_1} - \frac{2\rho q_1 q_2}{\sqrt{4\lambda_1\lambda_2}} + \frac{q_2^2}{2\lambda_2}\right) \quad (1)$$

where $\rho = \lambda_{12}/(\lambda_1\lambda_2)^{1/2}$ is the coordinate correlation coefficient, λ_1 and λ_2 are the solvent reorganization energies for electron transfer along q_1 and q_2 coordinates and λ_{12} is a measure of the coordinate correlation. The reorganization energies measure the standard deviations of the reaction coordinates. The standard deviations are given by $\Delta_1^2 = \langle \delta q_1(0)\,\delta q_1(0)\rangle_{av}$, $\Delta_2^2 = \langle \delta q_2(0)\,\delta q_2(0)\rangle_{av}$ and $\Delta_{12}^2 = \langle \delta q_1(0)\,\delta q_2(0)\rangle_{av}$ measures the equilibrium correlation of the reaction coordinates. The following relations hold: $\Delta_1^2 = 2\lambda_1 k_B T$, $\Delta_2^2 = 2\lambda_2 k_B T$ and $\Delta_{12}^2 = 2\lambda_{12} k_B T$.

Within the framework of the linear response theory, the potential energy surfaces for the charge transfer (CT) states $D^+-A_1^-A_2$ and $D^+-A_1-A_2^-$ are given by [18,24,25]

$$U_2(q_1,q_2) = U_1(q_1,q_2) - q_1 + \lambda_1 + \Delta G_{12} \quad (2)$$

and

$$U_3(q_1,q_2) = U_1(q_1,q_2) - q_1 + q_2 + \lambda_3 + \Delta G_{13} \quad (3)$$

respectively. The combined reorganization energy for the 1 to 3 transition is given by $\lambda_3 = \lambda_1 + \lambda_2 - 2\lambda_{12}$. The minimum of the surface $U_2(q_1,q_2)$ is located at $q_1^{(2)} = 2\lambda_1$, $q_2^{(2)} = 2\lambda_{12}$; the minimum of the surface $U_3(q_1,q_2)$ is at $q_1^{(3)} = 2\lambda_1 - 2\lambda_{12}$, $q_2^{(3)} = -2\lambda_2 + 2\lambda_{12}$. The contour maps of the potential energy surfaces 1–3 are shown in Fig. 1.

The distribution function of the solvent polarization coordinates at equilibrium is given by

$$\phi^{eq}(q_1,q_2) = \frac{1}{2\pi\Delta_1\Delta_2\sqrt{1-\rho^2}} \times \exp\left[-\frac{1}{2(1-\rho^2)}\left(\frac{q_1^2}{\Delta_1^2} - 2\rho\frac{q_1 q_2}{\Delta_1\Delta_2} + \frac{q_2^2}{\Delta_2^2}\right)\right] \quad (4)$$

where $\rho = \Delta_{12}^2/[\Delta_1\Delta_2]$.

The solvation dynamics can be described in terms of Green's function $\phi(q_1,q_2,t|q_1^0,q_2^0)$ representing the conditional probability that the solvation coordinates have expectation values q_1,q_2 at time t given that they had the values q_1^0,q_2^0 at time 0 if the system is in the single electronic state. The derivation of the equation for Green's function using cumulant expansion to the second order is presented elsewhere [27]. The dynamic correlations are described using the following matrix

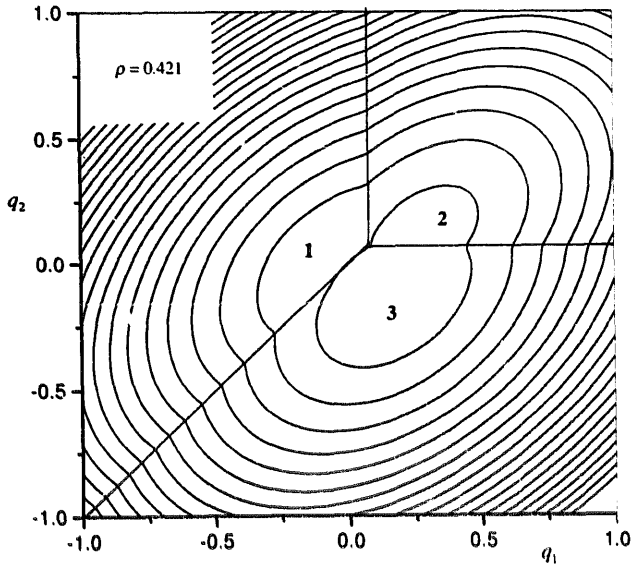

Fig. 1. Potential energy contour maps ($\Delta U_i = 0.2$ eV) for the lowest energy surfaces. $\Delta G_{12} = -0.075$ eV, $\Delta G_{13} = -0.15$ eV, $\lambda_1 = 0.1432$ eV, $\lambda_2 = 0.1272$ eV, $\lambda_3 = 0.1567$ eV. The reorganization energies were derived from the molecular dynamics simulations for the photosynthetic reaction centre by Marchi et al. [3].

$$\mathbf{S}(t) = \begin{bmatrix} \Delta_1^2 & \Delta_{12}^2 & \Delta_1^2 M_1(t) & \Delta_{12}^2 M_{12}(t) \\ \Delta_{12}^2 & \Delta_2^2 & \Delta_{12}^2 M_{12}(t) & \Delta_2^2 M_2(t) \\ \Delta_1^2 M_1(t) & \Delta_{12}^2 M_{12}(t) & \Delta_1^2 & \Delta_{12}^2 \\ \Delta_{12}^2 M_{12}(t) & \Delta_2^2 M_2(t) & \Delta_{12}^2 & \Delta_2^2 \end{bmatrix} \tag{5}$$

The matrix $\mathbf{S}(t)$ is a symmetric matrix of the auto-correlation and cross-correlation functions and the corresponding standard deviations. The auto-correlation functions are defined as $M_1(t) = \langle \delta q_1(t)\,\delta q_1(0)\rangle_{av}/\Delta_1^2$, $M_2(t) = \langle \delta q_2(t)\,\delta q_2(0)\rangle_{av}/\Delta_2^2$. The cross-correlation function is normalized as follows $M_{12}(t) = \langle \delta q_1(t)\,\delta q_2(0)\rangle_{av}/\Delta_{12}^2$.

Green's function $\phi(q_1,q_2,t|q'_1,q'_2)$ for the neutral state of the triad system has the following form

$$\phi(x_1,x_2,t|x_3,x_4) = \frac{1}{2\pi\sqrt{|\mathbf{S}(t)|}} \times \exp\left[-\frac{1}{2}\sum_{l,k}^{4} x_l S_{lk}^{-1}(t) x_k\right] \Big/ \phi^{eq}(x_3,x_4) \tag{6}$$

The matrix elements of the inverse matrix $\mathbf{S}^{-1}(t)$ are calculated using the standard procedure

$$S_{lk}^{-1}(t) = (-1)^{l+k} |\mathbf{S}^{T}(t)_{lk}| / |\mathbf{S}(t)| \tag{7}$$

where $|\mathbf{S}^{T}(t)_{lk}|$ is the determinant of the minor $\mathbf{S}^{T}(t)_{lk}$ obtained from the transposed $\mathbf{S}(t)$ matrix by removing the lth row and kth column. The determinant $|\mathbf{S}(t)|$ of the matrix $\mathbf{S}(t)$ is equal to

$$\begin{aligned} |\mathbf{S}(t)| = \Delta_{12}^4 \Delta_{23}^4 \{ & [1 - M_1^2(t)] \\ & \times [1 - M_2^2(t)] + \rho^4 [1 - M_{12}^2(t)]^2 \\ & - 2\rho^2 [[1 + M_1(t) M_2(t)][1 + M_{12}^2(t)] \\ & - 2M_{12}(t)[M_1(t) + M_2)]] \} \end{aligned} \tag{8}$$

At long times, Green's function reaches the equilibrium distribution in a particular state $\phi(q_1,q_2,t|q_1^0,q_2^0) \rightarrow \phi^{eq}(q_1,q_2)$.

Both the experimental data and theoretical predictions, e.g. the results of molecular dynamics simulations, show that the auto-correlation functions $M_j(t)$ are non-exponential functions of time [3,4,14,28–31]. At very short times, the inertial effects determine the time dependence of the auto-correlation function. In the general case, the dynamics of the system can be characterized using suitably chosen auto- and cross-correlation functions of system variables. These functions can be calculated using, for example, the methods of molecular dynamics. The simulations performed by Marchi et al. [3] for the triad system composed of the special pair, bacteriochlorophyll and bacteriopheophytin in the bacterial photosynthetic reaction centre of *Rhodopseudomonas viridis* showed that the fluctuations in the two energy gaps are correlated.

Within the framework of the linear response theory, Green's functions for different electronic states are given by [18,24]

$$\begin{aligned} & \phi_m(q_1,q_2,t|q_1^0,q_2^0) \\ & \quad = \phi(q_1 - q_1^{(m)}, q_2 - q_2^{(m)}, t | q_1^0 - q_1^{(m)}, q_2^0 - q_2^{(m)}) \end{aligned} \tag{9}$$

where $q_1^{(m)}$, $q_2^{(m)}$ specify the position of the minimum of the surface m. The Green's functions given by Eqs. (6) and (9) describe the dynamics on each surface in the absence of electron transfer processes. They are considered as the solutions of the equations of the following general type [32,33]

$$\frac{\partial}{\partial t}\phi_m(q_1,q_2,t) = \Gamma_{mm}^{D}(q_1,q_2,t) \circ \phi_m(q_1,q_2,t) \tag{10}$$

for the initial distribution $\phi_m(q_1,q_2,0) = \delta(q_1 - q_1^0)\,\delta(q_2 - q_2^0)$. The form of the integro-differential operator $\Gamma_{mm}^{D}\circ$ is considered to be quite general. In the Laplace domain we have

$$\begin{aligned} & s\bar{\phi}_m(q_1,q_2,s|q_1^0,q_2^0) - \phi(q_1,q_2,0) \\ & \quad = L[\Gamma_{mm}^{D}(q_1,q_2,t) \circ \phi_m(q_1,q_2,t|q_1^0,q_2^0)] \end{aligned} \tag{11}$$

where L[...] denotes the Laplace transformation.

The Laplace transforms of Green's functions can also be given by [32–35]

$$\bar{\phi}_n(q_1,q_2,s|1_1^0,q_2^0) = \frac{\phi_n^{eq}(q_1,q_2)}{s} + \phi_n^{eq}(0,0)\,\bar{\tau}_n(q_1,q_2,s|q_1^0,q_2^0) \tag{12a}$$

$$\bar{\tau}_n(q_1,q_2,s|q_1^0,q_2^0) = \frac{1}{\phi_n^{eq}(0,0)}\int_0^\infty [\phi_n(q_1,q_2,t|q_1^0,q_2^0) - \phi_n^{eq}(q_1,q_2)] \times \exp(-st)\,dt \quad (12b)$$

where $\bar{\tau}(q_1,q_2,s|\ q_1^0,q_2^0)$ represents the solvent relaxation time scale functions. In Green's function (12a), the first term describes the equilibrium contribution, whereas the second is due to the finite rate of the solvation dynamics in the given electronic state.

3. Stochastic Liouville equations for the triad system

The stochastic Liouville equation for the density matrix of the three-level system (which includes the solvation dynamics in the supramolecular three-component system in a polar solvent) has the following form [6,9]

$$\frac{\partial}{\partial t}\rho(q_1,q_2,t) = -\frac{i}{\hbar}[\mathrm{H}(q_1,q_2,t),\rho(q_1,q_2,t)] + \frac{\partial}{\partial t}\rho(q_1,q_2,t)|_{rel} \quad (13)$$

where the system hamiltonian is given by

$$\mathrm{H}(q_1,q_2,t) = \begin{bmatrix} U_1(q_1,q_2) & V_{12} & V_{13} \\ V_{12} & U_2(q_1,q_2) & V_{23} \\ V_{13} & V_{23} & U_3(q_1,q_2) \end{bmatrix} \quad (14)$$

Here V_{mn} are the electronic coupling matrix elements between the diabatic potential energy surfaces $U_m(q_1,q_2)$ and $U_n(q_1,q_2)$. We use the following notation $U_{mn} = U_m(q_1,q_2) - U_n(q_1,q_2)$ for the vertical energy differences. The following relation holds: $U_{12} + U_{23} = U_{13}$.

The relaxation term in Eq. (13) accounts for the solvation dynamics on three surfaces (diagonal terms) and phenomenologically the dephasing for the off-diagonal elements of the density matrix (as in optical Bloch equations) [6]

$$\frac{\partial}{\partial t}\rho(q_1,q_2,t)|_{rel} = \begin{bmatrix} \Gamma_{11}^D \circ \rho_{11} & -\Gamma_{12}\rho_{12} & -\Gamma_{13}\rho_{13} \\ -\Gamma_{21}\rho_{21} & \Gamma_{22}^D \circ \rho_{22} & -\Gamma_{23}\rho_{23} \\ -\Gamma_{31}\rho_{31} & -\Gamma_{32}\rho_{32} & \Gamma_{33}^D \circ \rho_{33} \end{bmatrix} \quad (15)$$

The form of the hamiltonian and the relaxation term imply that, in the present formulation, we can model both the static limit of the solvent fluctuations considered by Hu and Mukamel [6,7] and to some extent the dephasing of electronic coherence. We assume that $\Gamma_{mn} = \Gamma_{nm}$. The relaxation of the diagonal elements of the density matrix (populations), i.e. the solvation dynamics, is described by Eqs. (6) and (9). The matrix elements of the density in the frequency domain satisfy the following equations

$$s\bar{\rho}_{mn} - \rho_{mn}(0) = -\frac{i}{\hbar}[\mathrm{H},\bar{\rho}]_{mn} + \mathrm{L}[\partial\rho_{mn}/\partial t|_{rel}],\quad m,n = 1, 2, 3 \quad (16)$$

In an explicit form the Liouville equation represents nine equations for the Laplace transforms of the elements of the density matrix.

Using the solutions for the off-diagonal matrix elements, the kinetic equations for the populations of the three levels in the Laplace domain can be written in terms of the three rate functions [34–36]

$$s\bar{\rho}_{11}(q_1,q_2,s) - \rho_{11}(0) = -\bar{F}_1(q_1,q_2,s) - \bar{F}_2(q_1,q_2,s) + \Gamma_{11}^D\bar{\rho}_{11}(q_1,q_2,s) \quad (17a)$$

$$s\bar{\rho}_{22}(q_1,q_2,s) = +\bar{F}_1(q_1,q_2,s) - \bar{F}_3(q_1,q_2,s) + \Gamma_{22}^D\bar{\rho}_{22}(q_1,q_2,s) \quad (17b)$$

$$s\bar{\rho}_{33}(q_1,q_2,s) = +\bar{F}_2(q_0,q_2,s) + \bar{F}_3(q_1,q_2,s) + \Gamma_{33}^D\bar{\rho}_{33}(q_1,q_2,s) \quad (17c)$$

The rate functions have been defined as follows

$$\bar{F}_1(q_1,q_2,s) = \bar{K}_1(q_1,q_2,s)[\bar{\rho}_{11}(q_1,q_2,s) - \bar{\rho}_{22}(q_1,q_2,s)] \quad (18a)$$

$$\bar{F}_2(q_1,q_2,s) = \bar{K}_2(q_1,q_2,s)[\bar{\rho}_{11}(q_1,q_2,s) - \bar{\rho}_{33}(q_1,q_2,s)] \quad (18b)$$

$$\bar{F}_3(q_1,q_2,s) = \bar{K}_3(q_1,q_2,s)[\bar{\rho}_{22}(q_1,q_2,s) - \bar{\rho}_{33}(q_1,q_2,s)] \quad (18c)$$

where the functions $\bar{K}_l(q_1,q_2,s)$ play the role of the effective coupling between the donor and acceptor sites. Detailed equations for the coupling functions will be given elsewhere (see also Appendix A). Below, we consider specific examples and approximations for $\bar{K}_l(q_1,q_2,s)$. In the general case, the effective coupling function contains contributions due to the direct coupling of the two states and due to superexchange. The functions $\bar{K}_l(q_1,q_2,s)$ have large values along the intersections of the potential energy functions.

The solutions of the kinetic equations for the populations of the levels in the Laplace domain in terms of the gaussian wavepackets are as follows [32,36]

$$\bar{\rho}_{11}(q_1,q_2,s) = \iint\rho_{11}(q_1^0,q_2^0,0)\bar{\phi}_1(q_1,q_2,s|q_1^0,q_2^0)dq_1^0dq_2^0 - \iint\bar{F}_1(q_1^0,q_2^0,s)\bar{\phi}_1(q_1,q_2,s|q_1^0)dq_1^0dq_2^0 - \iint\bar{F}_2(q_1^0,q_2^0,s)\bar{\phi}_1(q_1,q_2,s|q_1^0,q_2^0)dq_1^0dq_2^0 \quad (19a)$$

$$\bar{\rho}_{22}(q_1,q_2,s) = +\iint\bar{F}_1(q_1^0,q_2^0,s)\bar{\phi}_2(q_1,q_2,s|q_1^0,q_2^0)dq_1^0dq_2^0 - \iint\bar{F}_3(q_1^0,q_2^0,s)\bar{\phi}_2(q_1,q_2,s|q_1^0,q_2^0)dq_1^0dq_2^0 \quad (19b)$$

$$\bar{\rho}_{33}(q_1,q_2,s) = + \int\int \bar{F}_2(q_1^0,q_2^0,s)\bar{\phi}_3(q_1,q_2,s|q_1^0,q_2^0)\mathrm{d}q_1^0\mathrm{d}q_2^0 + \int\int \bar{F}_3(q_1^0,q_2^0,s)\bar{\phi}_3(q_1,q_2,s|q_1^0,q_2^0)\mathrm{d}q_1^0\mathrm{d}q_2^0 \quad (19c)$$

The first term in Eq. (19a) depends on the initial distribution of the population on surface 1. For photoinduced electron transfer processes this distribution is established by the photoexcitation mode. Transient hole burning experiments show that this distribution can be controlled by the properties of the laser pulses. Here, for simplicity, we assume that the initial distribution on surface 1 is the equilibrium gaussian distribution. For the initial equilibrium distribution $\rho_{11}(q_1^0,q_2^0,0) = \phi_1^{eq}(q_1^0,q_2^0)$, we have

$$\int\int \rho_{ini}(q_1^0,q_2^0,0)\bar{\phi}_1(q_1,q_2,s|q_1^0,q_2^0)\mathrm{d}q_1^0\mathrm{d}q_2^0 = \phi_1^{eq}(q_1,q_2)/s \quad (20)$$

We note that $\phi_1^{eq}(q_1,q_2)$ also represents the long time limit of the gaussian function $\phi_1(q_1,q_2,t|q_1^0,q_2^0)$.

The total populations of the three levels in the Laplace domain can be obtained by integrating the populations $\bar{\rho}_{mm}(q_1,q_2)$ over the solvent polarization coordinates

$$\bar{\rho}_{mm}(s) = \int\int \bar{\rho}_{mm}(q_1,q_2)\mathrm{d}q_1\mathrm{d}q_2 \quad (21)$$

Using Eqs. (19) and (21), these populations can be expressed as

$$\bar{\rho}_{11}(s) = \frac{1}{s}[1 - \bar{F}_1(s) - \bar{F}_2(s)] \quad (22a)$$

$$\bar{\rho}_{22}(s) = \frac{1}{s}[\bar{F}_1(s) - \bar{F}_3(s)] \quad (22b)$$

$$\bar{\rho}_{33}(s) = \frac{1}{s}[\bar{F}_2(s) + \bar{F}_3(s)] \quad (22c)$$

where

$$\bar{F}_m(s) = \int\int \bar{F}_m(q_1,q_2,s)\mathrm{d}q_1\mathrm{d}q_2 \quad (23)$$

represents the total rate functions for the transitions in the three-level system. Using Eqs. (18) defining the rate functions, the formal solutions for the populations of the states (Eqs. (19)) and integrating over the coordinate space, we obtain the integral equations for the total rate functions

$$\begin{aligned}\bar{F}_1(s) = \frac{1}{s}\{&\bar{Q}_{11}(s) - \bar{F}_1(s)[\bar{Q}_{11}(s) + \bar{Q}_{12}(s)] \\ &- \bar{F}_2(s)\bar{Q}_{11}(s) + F_3(s)\bar{Q}_{12}(s)\} \\ &- \int\int F_1(q_1^0,q_2^0,s)[\bar{T}_{11}(q_1^0,q_2^0,s) \\ &+ \bar{T}_{12}(q_1^0,q_2^0,s)]\mathrm{d}q_1^0\mathrm{d}q_2^0 \\ &- \int\int \bar{F}_2(q_1^0,q_2^0,s)\bar{T}_{11}(q_1^0,q_2^0,s)\mathrm{d}q_1^0\mathrm{d}q_2^0 \\ &+ \int\int \bar{F}_3(q_1^0,q_2^0,s)\bar{T}_{12}(q_1^0,1_2^0,s)\mathrm{d}q_1^0\mathrm{d}q_2^0 \end{aligned} \quad (24a)$$

$$\begin{aligned}F_2(s) = \frac{1}{s}\{&\bar{Q}_{21}(s)\bar{Q}_{21}(s) - \bar{F}_2(s)[\bar{Q}_{21}(s) \\ &+ \bar{Q}_{23}(s)] - F_3(s)\bar{Q}_{23}(s)\} \\ &- \int\int [\bar{F}_1(q_1^0,q_2^0,s)\bar{T}_{21}(q_1^0,q_2^0,s)\mathrm{d}q_1^0\mathrm{d}q_2^0 \\ &- \int\int \bar{F}_2(q_1^0,q_2^0,s)[\bar{T}_{21}(q_1^0,q_2^0,s) \\ &+ \bar{T}_{23}(q_1^0,q_2^0,s)]\mathrm{d}q_1^0\mathrm{d}q_2^0 \\ &- \int\int \bar{F}_3(q_1^0,q_2^0,s)\bar{T}_{23}(q_1^0,q_2^0,s)]\mathrm{d}q_1^0\mathrm{d}q_2^0 \end{aligned} \quad (24b)$$

$$\begin{aligned}F_3(s) = \frac{1}{s}\{&\bar{F}_1(s)\bar{Q}_{32}(s) - F_2(s)\bar{Q}_{33}(s) \\ &- \bar{F}_3(s)[\bar{Q}_{32}(s) + \bar{Q}_{33}(s)]\} \\ &+ \int\int \bar{F}_1(q_1^0,q_2^0,s)\bar{T}_{32}(q_1^0,q_2',s)\mathrm{d}q_1^0\mathrm{d}q_2^0 \\ &- \int\int \bar{F}_2(q_1^0,q_2^0,s)\bar{T}_{33}(q_1^0,q_2^0,s)\mathrm{d}q_1^0\mathrm{d}q_2^0 \\ &- \int\int \bar{F}_3(q_1^0,q_2^0,s)[\bar{T}_{32}(q_1^0,q_2^0,s) \\ &+ \bar{T}_{33}(q_1^0,q_2^0,s)]\mathrm{d}q_1^0\mathrm{d}q_2^0 \end{aligned} \quad (24c)$$

where

$$\bar{Q}_{mn}(s) = \int\int \bar{K}_m(q_1,q_2,s)\phi_n^{eq}(q_1,q_2)\mathrm{d}q_1\mathrm{d}q_2 \quad (25a)$$

and

$$\bar{T}_{mn}(q_1^0,q_2^0,s) = \phi_n^{eq}(0,0)\int\int \bar{K}_m(q_1,q_2,s)\bar{\tau}_n(q_1,q_2,s|q_1^0,q_2^0)\mathrm{d}q_1\mathrm{d}q_2 \quad (25b)$$

The integral terms represent the double overlap of the solvent time scale functions $\bar{\tau}_n(q_1,q_2,s|q_1^0,q_2^0)$ and the two functions $\bar{K}_m(q_1,q_2,s)$ and $\bar{F}_l(q_1^0,q_2^0,s)$. The three integrals $\int\int\int\int \bar{F}_l(q_1^0,q_2^0,s)[\bar{\tau}_m(q_1, q_2s|q_1^0, q_2^0) + \bar{\tau}_n(q_1, q_2,s|q_1^0q_2^0)] \bar{K}_l(q_1,q_2,s)\,\mathrm{d}q_1^0\mathrm{d}q_1\mathrm{d}q_2$ give the measure of the adiabaticity of the electron transfer at the intersection of the surfaces m and n. The six integrals $\int\int\int\int \bar{F}_l(q_1^0,q_2^0,1)\bar{\tau}_m q_1,q_2,s|q_1^0,q_2^0) \bar{K}_k(q_1,q_2,s)\mathrm{d}q_1^0,\mathrm{d}q_2^0\mathrm{d}q_1\mathrm{d}q_2$ describe the dynamic coupling of the electron transfer processes occurring along different intersections, l and k, due to the finite rate of wavepacket propagation on the surface m.

Since the functions $\bar{K}_m(q_1,q_2,s)$ are defined by explicit expressions, finding a solution to Eqs. (24) is equivalent to finding a self-consistent population difference between the reactant and product states. An iterative approach to the solution of the integral equations can be used. Moreover, Eqs. (24) can also be used as a convenient starting point for various approximation schemes.

The kinetic description of the electron transfer processes in the three-level system developed here can be applied to a

variety of physical systems. In particular, the non-adiabatic limit of the electron transfer processes in the triad system holds when all solvent time scale functions are vanishing $\bar{\tau}_n(q_1,q_2,s|q_1^0,q_2^0) \approx 0$. In this limiting case, all integral terms containing the functions $\bar{T}_{mn}(q_1^0,q_2^0,s)$ vanish, and we obtain a set of algebraic equations for the Laplace transforms of the rate functions $\bar{F}_n(s)$. Namely, Eqs. (24) simplify as follows

$$\left\{\begin{bmatrix} \bar{Q}_{11}(s)+\bar{Q}_{12}(s) & \bar{Q}_{11}(s) & -\bar{Q}_{12}(s) \\ \bar{Q}_{21}(s) & \bar{Q}_{21}(s)+\bar{Q}_{23}(s) & \bar{Q}_{23}(s) \\ -\bar{Q}_{32}(s) & \bar{Q}_{33}(s) & \bar{Q}_{32}(s)+\bar{Q}_{33}(s) \end{bmatrix} + s\begin{bmatrix} 1 & 0 & 0 \\ 0 & 1 & 0 \\ 0 & 0 & 1 \end{bmatrix}\right\} \begin{bmatrix} \bar{F}_1(s) \\ \bar{F}_2(s) \\ \bar{F}_3(s) \end{bmatrix} = \begin{bmatrix} \bar{Q}_{11}(s) \\ \bar{Q}_{21}(s) \\ 0 \end{bmatrix} \tag{26}$$

The solution of the coupled equation (Eq. (26)) can be obtained using standard algebraic methods, e.g. by constructing the inverse matrix to the matrix on the left-hand side of Eq. (26). Eq. (26) represents an important result of the present formulation of the outer-sphere electron transfer in the triad system. The superexchange mechanism of electron transfer and resonance tunnelling effects in the non-adiabatic limit can be modelled using these equations.

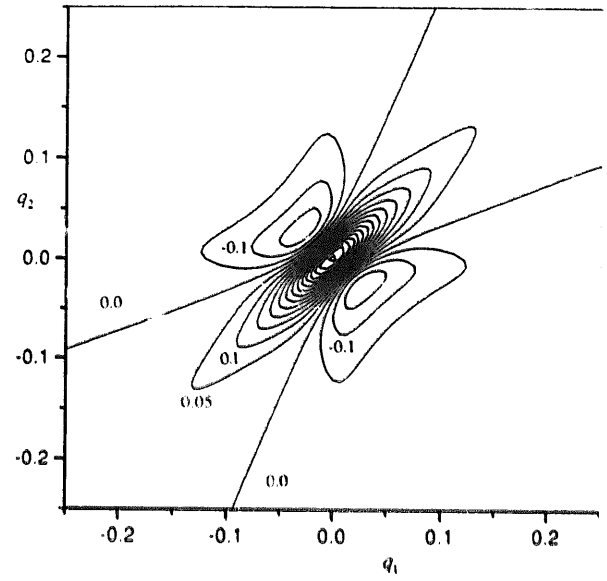

Fig. 2. Contour map for the effective coupling function $\bar{K}(q_1,q_2,\Gamma) = v_{12}v_{23}\bar{S}_2(q_1,q_2,\Gamma)$. The coordinate origin is at the common point of the three intersection lines between the pairs of the potential energy function. $V_{12} = V_{23} = 0.01$ eV. The function assumes positive values along the intersection between the surfaces 1 and 3. In the perpendicular direction, the function reaches negative values with two minima. The contour line spacing is 0.05 eV ps^{-1}.

4. Modelling of the photosynthetic reaction centre

For the photosynthetic reaction centre, the distance between the donor D and the second acceptor A_2 is large. The corresponding electronic coupling matrix element is expected to be very small $V_{13} \cong 0$ [2,5,7,8]. The functions $\bar{K}_l(q_1,q_2,s)$ for this particular situation are given in Appendix A. We can distinguish two situations.

(1) When $V_{ik} = 0$, the dominant contribution to the effective coupling between the states l and k is due to coupling of the initial and final states through the intermediate state $s \neq l$, $s \neq k$. In the case of the superexchange mechanism, $\bar{K}_X(q_1,q_2,s)$ shows a strong dependence on both reaction coordinates. The function reaches a maximum at the point common to the three intersection lines. Moreover, along the direction of the two other intersection lines it attains negative values. The contour plots of $\bar{K}_2(q_1,q_2,s)$ are shown in Fig. 2 for the dephasing $\Gamma_{ik} = 50$ fs^{-1}. This value is used for visualization purposes only. With increasing dephasing rate, the effective coupling function $\bar{K}_2(q_1,q_2,s) = V_{12}V_{23}\bar{S}_2(q_1,q_2,s)/\hbar^2$ decreases and spreads over a large area in the coordinate space. In Appendix A, a Zusman-type approximation [37] for the effective coupling function $\bar{K}_2(q_1,q_2,s)$ is given. The matrix elements $\bar{Q}_{21}(0)$ and $\bar{Q}_{23}(0)$ can be evaluated by numerical methods using Eqs. (25) and (A8).

(2) When $V_{ik} \neq 0$, the dominant contribution is due to direct coupling between the states l and k. The corresponding rate functions $\bar{K}_X(q_1,q_2,s)$ can be given in the following form using approximations proposed by Zusman [37]

$$\bar{K}_X(q_1,q_2,s) = \frac{V_{ik}^2}{\hbar^2}\bar{P}_X(q_1,q_2,s) - \frac{V_{12}V_{23}}{\hbar^2}\bar{S}_X(q_1,q_2,s)$$

$$\cong \frac{2\pi V_{ik}^2}{\hbar}\delta(U_{ik}) - \frac{V_{12}V_{23}}{\hbar^2}\bar{S}_X(q_1,q_2,s) \tag{27}$$

Using approximations (27) and (A8), we obtain for the matrix elements

$$\bar{Q}_{11}(0) \cong \frac{2\pi V_{12}^2}{\hbar\sqrt{4\pi\lambda_1 k_B T}} \times \exp\left[-\frac{(\lambda_1+\Delta G_{12})^2}{4\lambda_1 k_B T}\right] - \bar{Q}_{21}(0) \tag{28a}$$

$$\bar{Q}_{32}(0) \cong \frac{2\pi V_{23}^2}{\hbar\sqrt{4\pi\lambda_2 k_B T}} \times \exp\left[-\frac{(\lambda_2+\Delta G_{13}-\Delta G_{12})^2}{4\lambda_2 k_B T}\right] - \bar{Q}_{21}(0) \tag{28b}$$

The relative contribution of the superexchange mechanism in the charge separation process can be quantitatively characterized using the functions $F_1(t)$ and $F_2(t)$. For simple comparison, we can use the following expression for the branching ratio at the steady state

$$B = \frac{\bar{Q}_{21}(0)}{\bar{Q}_{11}(0)+2\bar{Q}_{21}(0)} \tag{29}$$

Table 1
The time constants and free energies of primary electron transfer in the photosynthetic reaction centre of *Rhodobacter sphaeroides* [5]

Strain	τ(295 K) (ps)	τ(80 K) (ps)	ΔT_{13} (eV)
Wild type	3.5±0.3	1.7±0.2	−0.15±0.01
(M)Y210F	10.5±1.0	10.5±1.0	−0.11±0.01
(M)Y210I	16±2	55±5	−0.12±0.01
(M)Y210W	41±4	155±10	−0.09±0.01

Recently, Nagarajan et al. [5] have investigated the photoinduced electron transfer in the photosynthetic reaction centre of *Rhodobacter sphaeroides* in mutant strains in which tyrosine (M)210 is replaced by phenylalanine, isoleucine or tryptophan. Their results concerning the mean electron transfer time constants at room temperature (τ(295 K)) and at 80 K (τ(80 K)), and the free energies (ΔG_{13}(295 K)) of electron transfer from excited bacteriochlorophyll dimer (P^*) to bacteriopheophytin (H_L) are given in Table 1.

Nagarajan et al. [5] analysed their experimental results assuming sequential electron transfer using the potential energy surfaces in two strongly correlated reaction coordinates. They conclude that the temperature dependence of the electron transfer reaction in the mutants cannot be explained adequately on the assumption that the mutations only alter the overall ΔG_{13} values, but it can be accounted for by assuming that they also increase the free energy of the additional state ($P^+B_L^-$) that serves as both a kinetic and a virtual intermediate. The evaluated increases in the free energy of ($P^+B_L^-$) were found to be greater than the measured changes in the free energy of ($P^+H_L^-$).

The reorganization energies for separate electron transfer steps are important parameters for the modelling of the electron transfer rates in the triad system. Estimates of the reorganization energies for the photosynthetic reaction centre vary over one order of magnitude from 200 to 2000 cm^{-1} [1–3,5,9]. In the kinetic analysis, very different correlation coefficients of the reaction coordinates were assumed. In the present model, we employ parameters obtained by Marchi et al. [3] using molecular dynamics calculations for the photosynthetic reaction centre of *Rhodopseudomonas viridis*. The estimates (Eq. (29)) of the contribution of superexchange to the charge separation in the triad system for different values of the electron transfer free energies ΔG_{13} and ΔG_{12} are shown in Fig. 3. The upper part of Fig. 3 corresponds to the normal Marcus regime for (P^*) to ($P^+B_L^-$) electron transfer. Since the populations of the intermediate state are below the detection limits, the rate coefficient for electron transfer from ($P^+B_L^-$) to ($P^+H_L^-$) should be larger than that from (P^*) to ($P^+B_L^-$). This limits the possible range of the free energies. The free energies pertinent to photosynthetic reaction centres are shown in the middle. The contribution of the superexchange mechanism to the charge separation in this range of free energies is between 5% and 15%.

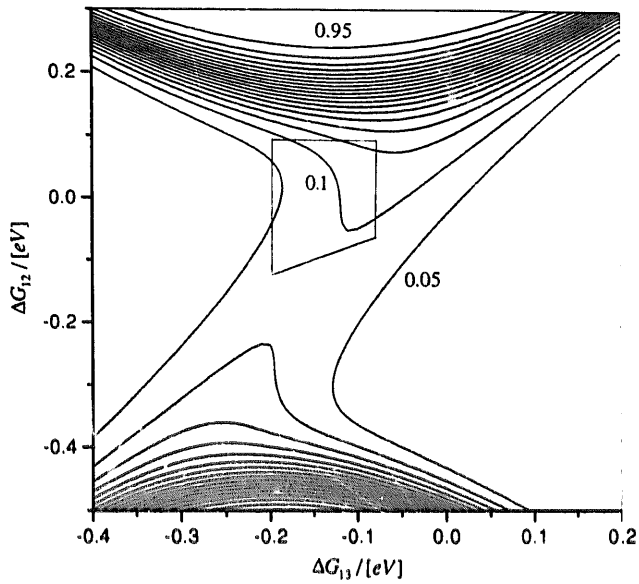

Fig. 3. The contour map for the function $B(\Delta G_1, \Delta G_2)$ ($\Delta B = 0.05$) characterizing the relative contributions of the superexchange mechanism to the decay of the initial state. Parameters as in Fig. 1, $V_{12} = V_{23} = 0.01$ eV. The saddle point is at the free energies corresponding to two barrierless electron transfer processes.

5. Conclusions

The theory of non-adiabatic electron transfer reactions based on the stochastic Liouville equation has been extended to triad systems, e.g. D–A–A. Distinctive features of the present formulation are the use of the potential energy functions for the three electronic states employing two mutually correlated solvent polarization coordinates. They describe the influence of the solvent on the energy levels of the electronic states participating in the electron transfer processes. The characteristics of the dynamic processes are determined by potential barriers as well as the friction at the molecular level.

The dynamic response of the solvent is described using the auto-correlation functions for each solvent polarization coordinate. The solvent relaxation time spectrum can be properly included in the model. The time evolution of the supramolecular system has been described using gaussian wavepackets propagating on the three potential energy surfaces. In a certain region of the solvent polarization coordinate space, the three states are degenerate. At this stage of solvent polarization fluctuations, resonance electron transfer occurs. The interplay between the sequential and superexchange processes has been investigated for different free energies of the electron transfer reaction.

Acknowledgements

This work was supported by the Science and Technology Agency of Japan.

Appendix A

The dependence of the effective coupling functions $\bar{K}_l(q_1,q_2,s)$ on the reaction coordinates q_1, q_2 is due to the reaction coordinate dependence of the three vertical energy differences: $U_{12}=q_1-\lambda_1-\Delta G_{12}$, $U_{23}=-q_2+\lambda_1-\lambda_3+\Delta G_{12}-\Delta G_{13}$ and $U_{13}=q_1-q_2-\lambda_3-\Delta G_{13}$. In order to write the polynomials in possibly compact notation, we introduce the following notation abbreviations: $s_{12}=s+\Gamma_{12}$, $s_{13}=s+\Gamma_{13}$, $s_{23}=s+\Gamma_{23}$, $v_{lk}=V_{lk}/\hbar$, $u_{lk}=U_{lk}/\hbar$ and $|d_{lk}|^2=(s+\Gamma_{lk})^2+U_{lk}^2/\hbar^2=s_{lk}^2+u_{lk}^2$. The effective coupling functions $\bar{K}_l(q_1,q_2,s)$ can be given in terms of the functions connected with the direct population transfer $\bar{P}_l(q_1,q_2,s)$ and the superexchange $\bar{S}_l(q_1,q_2,s)$. For the particular case $v_{13}=0$, we have

$$\bar{K}_1(q_1,q_2,s)=v_{12}^2\bar{P}_1(q_1,q_2,s)-v_{12}v_{23}\bar{S}_2(q_1,q_2,s) \quad \text{(A1a)}$$

$$\bar{K}_2(q_1,q_2,s)=v_{12}v_{23}\bar{S}_2(q_1,q_2,s) \quad \text{(A1b)}$$

$$\bar{K}_3(q_1,q_2,s)=v_{23}^2\bar{P}_3(q_1,q_2,s)-v_{12}v_{23}\bar{S}_2(q_1,q_2,s) \quad \text{(A1c)}$$

Let us denote the determinant of the set of equations for the off-diagonal matrix elements of the density matrix by $D(s)$. For $v_{13}=0$, it is given by

$$D(s)=|d_{12}|^2|d_{13}|^2|d_{23}|^2+2v_{12}^2|d_{12}|^2(s_{12}s_{23}-u_{13}u_{23})+2v_{12}^2v_{23}^2(s_{12}s_{23}+u_{12}u_{23})+2v_{23}^2|d_{23}|^2(s_{12}s_{13}-u_{13}u_{12})+v_{12}^4|d_{12}|^2+v_{23}^4|d_{23}|^2 \quad \text{(A2)}$$

The functions $\bar{P}_1(q_1,q_2,s)$ and $\bar{P}_3(q_1,q_2,s)$ are as follows

$$\bar{P}_1(q_1,q_2,s)=2[s_{12}|d_{132}|^2|d_{23}|^2+2s_{12}v_{12}^2(s_{13}s_{23}-u_{13}u_{23})+v_{23}^2|d_{23}|^2s_{13}+v_{12}^2v_{23}^2s_{23}+v_{12}^4s_{12}]/D(s) \quad \text{(A3)}$$

$$\bar{P}_3(q_1,q_2,s)=2[s_{23}|d_{12}|^2|d_{13}|^2+2s_{23}v_{23}^2(s_{12}s_{13}-u_{12}u_{13})+v_{12}^2|d_{12}|^2s_{13}+v_{12}^2v_{23}^2s_{12}+v_{23}^4s_{23}]/D(s) \quad \text{(A4)}$$

The function $\bar{S}_2(q_1,q_2,s)$ is given by

$$\bar{S}_2(q_1,q_2,s)=2\{v_{12}v_{23}[s_{12}s_{13}s_{23}-s_{23}u_{12}u_{13}-s_{13}u_{12}u_{23}-s_{12}u_{13}u_{23}]+v_{12}^3v_{23}s_{12}+v_{23}^3v_{12}s_{23}\}/D(s) \quad \text{(A5)}$$

Along the intersection $u_{13}=0$, the following equalities hold: $u_{23}=-u_{12}$ and $q_2=q_1+C$, where $C=-\lambda_3-\Delta G_{13}$. The function $\bar{S}_2(q_1,q_1+C,s)$ is given by

$$\bar{S}_2(q_1,q_1+C,s)=2s_{13}v_{12}v_{23}[|d_{12}|^2+v_{12}^2+v_{23}^2]/D(s) \quad \text{(A6)}$$

where

$$D(s)\cong|d_{13}|^2\{|d_{12}|^4+|d_{12}|^2[2(v_{12}^2+v_{23}^2)+(v_{12}^2-v_{23}^2)^2/\Gamma^2]+4v_{12}^2v_{23}^2\} \quad \text{(A7)}$$

In deriving Eqs. (A6) and (A7), we have assumed that $\Gamma_{12}=\Gamma_{13}=\Gamma_{23}=\Gamma$.

Using the approximation $2s/(\hbar^2s^2+U_{13}^2)\cong 2\pi\delta(U_{13})/\hbar$ for Eq. (A6), we obtain an estimate for the superexchange coupling between states 1 and 3

$$\bar{K}_2(q_1,q_2,s)=v_{12}v_{23}\bar{S}_2(q_1,q_2,s)\cong 2\pi\hbar\delta(U_{12})\frac{(v_{12}v_{23})^2[|d_{12}|^2+v_{12}^2+v_{23}^2]}{|d_{12}|^4+|d_{12}|^2[2(v_{12}^2+v_{23}^2)+(v_{12}^2-v_{23}^2)^2/\Gamma^2]+4v_{12}^2v_{23}^2} \quad \text{(A8)}$$

The approximation $2s/(\hbar^2s^2+U_{12}^2)\cong 2\pi\delta(U_{12})/\hbar$ was originally introduced by Zusman [37] in his theory of the electron transfer processes in a two-level system. Approximations (A6)–(A8) neglect the negative contributions to the effective coupling function shown in Fig. 2. A similar approximation has been proposed recently by Tang and Norris [9] for the effective coupling function for the superexchange.

References

[1] A. Warshel and W.W. Parson, *Annu. Rev. Phys. Chem.*, *42* (1991) 279.
[2] M. Bixon, J. Jortner and M.E. Michel-Beyerle, *Biochim. Biophys. Acta*, *1056* (1991) 301.
[3] M. Marchi, J.N. Gehlen, D. Chandler and M. Newton, *J. Am. Chem. Soc.*, *115* (1993) 4178.
[4] J.N. Gehlen, M. Marchi and D. Chandler, *Science*, *263* (1994) 499.
[5] V. Nagarajan, W.W. Parson, D. Davies and C.C. Schenk, *Biochimie*, *32* (1993) 12 324.
[6] Y. Hu and S. Mukamel, *J. Chem. Phys.*, *91* (1989) 6973.
[7] Y. Hu and S. Mukamel, in J. Jortner and B. Pullman (eds.), *Perspectives in Photosynthesis, The Jerusalem Symposia on Quantum Chemistry and Biochemistry*, Vol. 22, Kluwer Academic Publishers, Dordrecht, 1990, p. 171.
[8] A. Warshel, Z.T. Chu and W.W. Parson, *Science*, *246* (1989) 112.
[9] J. Tang and J. Norris, *J. Chem. Phys.*, *101* (1994) 5615.
[10] M. Fushiki and M. Tachiya, *J. Phys. Chem.*, *98* (1994) 10 762.
[11] S. Mukamel, *Adv. Chem. Phys.*, *70* (1988) 165.
[12] R.F. Loring, Y.J. Yan and S. Mukamel, *J. Chem. Phys.*, *87* (1987) 5840.
[13] S. Mukamel and Y.J. Yan, *Adv. Chem. Phys.*, *73* (1989) 579.
[14] M. Sparpaglione and S. Mukamel, *J. Chem. Phys.*, *88* (1988) 3263.
[15] S. Mukamel and R.F. Loring, *J. Opt. Soc. Am.*, *B3* (1986) 595.
[16] L.E. Fried and S. Mukamel, *Adv. Chem. Phys.*, *84* (1993) 435.
[17] Y.J. Yan and S. Mukamel, *J. Chem. Phys.*, *89* (1988) 5160.
[18] J. Najbar and M. Tachiya, *J. Phys. Chem.*, *98* (1994) 199.
[19] T. Motylewski, J. Najbar and M. Tachiya, Correlation between reaction coordinates for electron transfer in a supramolecular triad system, *J. Phys. Chem.*, submitted.
[20] J. Tang, Z. Wang and J. Norris, *J. Chem. Phys.*, *99* (1993) 979.
[21] J. Tang and J. Norris, *Chem. Phys.*, *175* (1993) 337.
[22] J. Tang, *Chem. Phys.*, *184* (1994) 39.
[23] J. Tang, *Chem. Phys.*, *189* (1994) 427.
[24] M. Tachiya, *J. Phys. Chem.*, *93* (1989) 7050.
[25] M. Tachiya, *J. Phys. Chem.*, *97* (1993) 5911.
[26] A.M. Kuznetov and J. Ulstrup, *Chem. Phys.*, *157* (1991) 25.
[27] J. Najbar and M. Tachiya, Intramolecular electron transfer processes in the supramolecular triad systems in polar media, to be submitted.
[28] M. Maroncellli, *J. Chem. Phys.*, *94* (1991) 2084.
[29] P.F. Barbara and W. Jarzeba, *Adv. Photochem.*, *15* (1990) 1.

[30] R.A. Marcus, Commemorative Issue, *J. Phys. Chem.*, *90* (1986) 3657.
[31] K.V. Mikkelsen and M.D. Todd, in Y. Gauduel and P. Rossky (eds.), *AIP Conference Proceedings 298, Ultrafast Reaction Dynamics and Solvent Effects, Royaumont, France, 1993*, AIP Press, New York, 1993, p. 435.
[32] I. Rips and J. Jortner, *J. Chem. Phys.*, *87* (1987) 2090, 6513.
[33] T. Fonseca, *J. Chem. Phys.*, *91* (1989) 2869.
[34] P. Gajdek, J. Najbar and A.M. Turek, *J. Photochem. Photobiol. A: Chem.*, *84* (1994) 113.
[35] J. Najbar, M. Boczar and A.M. Turek, *Polish J. Chem.*, *67* (1993) 1425.
[36] J. Najbar and W. Jarzeba, *Chem. Phys. Lett.*, *196* (1992) 504.
[37] L.D. Zusman, *Chem. Phys.*, *41* (1980) 295.